multiple ECLs and the interface of extracellular and transmembrane domains are responsible for the tight binding of AVC to CCR5.

Amino acid substitutions are likely to cause substantial conformational changes in ECLs - Substitutions of amino acid residues, which are involved in hydrogen bonding, appear to directly and indirectly disrupt the hydrogen bond networks observed (Fig. 3*A-B*). For example, Gly163, located in TM 4, does not interact directly with AVC, but is responsible for maintaining the shape of the binding cavity by its hydrogen bond interactions with Ser180 and Lys191 (Fig. 3*A*). Thus, the shape of the cavity is most likely altered with G163R substitution, and thereby AVC could lose critical interactions with ECL2 and TM5. In contrast, it was found that G163R exerts minimal effects on the binding of either SCH-C or TAK-779 to CCR5 (Table 1), potentially because these two inhibitors do not have direct hydrogen bond interactions with the ECL or ECL-TM interface.

As mentioned above, the carboxyl of AVC forms hydrogen bonds with Lys191 and Ser180 (Fig. 3*A*). The loss of binding with K191A substitution (Table 1) is likely due to the loss of the hydrogen bond with AVC as well as the altered shape of the cavity, which was confirmed by structural analysis of $CCR5_{K191A}$-AVC complex. Neither SCH-C nor TAK-779 forms hydrogen bonds with Lys191 (Fig. 5*A-B* and Fig. 6*A*), hence it is thought that K191A substitution does not significantly affect the binding affinity of SCH-C or TAK-779 (Table 1). Ile198 located in TM5 has hydrophobic interactions with AVC (Fig. 3*C*). SCH-C and TAK-779 were predicted to have hydrogen bond interactions with Tyr37 located in TM1 (Fig. 5*A-B* and Fig. 6*A-B*), while there appear to be no such interactions with AVC (Fig. 3*B*). This is consistent with the observation that the Y37A substitution drastically changed the binding affinity of SCH-C and TAK-779 to CCR5 (Table 1). Ile198 forms a hydrophobic contact with SCH-C (Fig. 5*C*) although not much with TAK-779, which well explains the reason I198A reduces the K_D value of SCH-C with CCR5 but not that of TAK-779 with CCR5 (Table 1). It is also of note that AVC has direct interactions with residues in the extracellular domain and its proximity (Cys178, Ser180, and Lys191)(Fig. 3*A-B*), which should strongly affect the conformation of extracellular loops in comparison to SCH-C and TAK-779, both of which failed to directly interact with the amino acid residues in the extracellular domain. The interaction of HIV-1-gp120 with ECLs is thought to be critical for the establishment of infection, therefore, one can assume that the binding of AVC to CCR5 should result in a significant loss of interactions with gp120, which could explain the significantly greater effect of AVC in blocking viral infectivity, compared to SCH-C and TAK-779.

Thus, the data above suggest the binding pockets are in the same general area within CCR5, however, the binding interactions of the three inhibitors with CCR5 residues substantially differ from each other, in particular between AVC and other two inhibitors.

Interactions between CCR5 inhibitors in relation to their binding to CCR5 - All three CCR5 inhibitors examined in this study possess the properties of allosteric antagonists of CCR5, while AVC exerts only partial inhibition of the binding to CCR5 and physiological function of ^{125}I-RANTES in comparison to TAK-779 and SCH-C (11). Moreover, although the binding pocket for these inhibitors are all located in the same hydrophobic cavity within CCR5, their binding profiles substantially differ from each other as discussed above. Therefore, we analyzed the interactions of the three inhibitors in relation to $CCR5_{WT}$. When $CCR5_{WT}$-CHO cells were exposed to ^{3}H-AVC (3 nM) for 15 minutes, followed by the addition of various concentrations (1 nM - 10 μM) of unlabelled SCH-C, ^{3}H-AVC binding to CCR5 was reduced only moderately, by up to 32% (Fig. 7*A*). When the interaction between ^{3}H-AVC and unlabelled TAK-779 (0.625 μM – 62.5 μM) was examined, ^{3}H-AVC binding to CCR5 was not significantly replaced by unlabelled TAK-779 (Fig. 7*B*). On the contrary, when ^{3}H-SCH-C was added first and then unlabelled AVC was added, the binding of ^{3}H-SCH-C to $CCR5_{WT}$-CHO cells was significantly blocked (Fig. 7*C*). These data suggest that AVC effectively replaces ^{3}H-SCH-C and binds to $CCR5_{WT}$. The binding of ^{3}H-TAK-779 was likewise blocked by the addition of unlabelled AVC, although the extent of replacement by AVC was lesser as compared to the case of ^{3}H-SCH-C (Fig. 7*D*).

Role of CCR5's amino acid residues with which aplaviroc is associated in HIV-1 infection and CC-chemokine binding - In an attempt to define the biological and virological roles of amino acid residues, with which AVC is associated in this binding to CCR5, we selected 15 mutant CCR5-overexpressing CHO cells and examined profiles of sCD4/gp120 binding and CC-chemokine (RANTES, MIP-1α, and MIP-1β) binding profile. Nine of the 15 mutants were chosen based on the following reasons. Tyr108 was chosen since Tyr108 is within the aromatic cluster seen in the proximity of TM2 and TM3 and is reported to play a crucial role in the CC-chemokine-elicited activation of CCR5 (35). Y37A and E283A were chosen since Tyr37 and Glu283 are involved in the binding of the three inhibitors to CCR5 and have been shown to be highly conserved in CC-chemokine receptors including CCR5, CCR2B, CCR3, CCR1, and CCR4 (6). Five more mutants (G163R, C178A, K191A, I198A, Y251A, and M287E) were also chosen, with which AVC's binding affinity was significantly reduced compared to $CCR5_{WT}$-expressing cells (>5-fold K_D difference)(Table 1). As shown in Fig. 8*A*, all the 9 mutations described above decreased the sCD4/gp120 binding to CCR5 compared to that to $CCR5_{WT}$. It was noted that Y108A, Y251A, and E283A substitutions resulted in the greatest reduction of sCD4/gp120 binding.

We further determined the binding profiles of ^{125}I-RANTES, ^{125}I-MIP-1α, and ^{125}I-MIP-1β to the above 9 mutant CCR5-overexpressing CHO cell lines (Fig. 8*B*). In several CHO cell lines, the CC-chemokine binding profile notably differed from the HIV-gp120/sCD4 complex binding profile. While both K191A and I198A substitutions caused moderate reduction in HIV-gp120/sCD4 complex binding (Fig. 8*A*), CC-chemokine binding was fairly preserved in $CCR5_{I198A}$-expressing cells while CC-chemokine binding was almost completely reduced in $CCR5_{K191A}$-expressing cells. The G163R substitution preserved HIV-gp120/sCD4 complex binding by 34%, however, CC-chemokine binding was substantially spared by 68 – 83%.

We also employed six additional mutant CCR5-overexpressing CHO cells, which showed insignificant to minimal changes (less than 3-fold differences) in their K_D values compared to K_D value for wild-type CCR5 (Table 1). Two substitutions in the extracellular domain of CCR5, D11A (NH_2-terminus) and KE171AA (ECL2), induced substantial reduction in HIV-gp120/sCD4 complex binding by 65 and 70%, respectively. The F112L, F112Y (both in TM3), S180T (ECL2) and M287A (TM7) substitutions caused no significant changes in K_D values (Table 1) or HIV-gp120/sCD4 complex binding (Fig 8*A*). These data suggest that amino acid residues in the proximity of the hydrophobic cavity for AVC that do not change K_D values generally do not affect the HIV-gp120/sCD4 complex binding to CCR5. These 6 substitutions, however, caused CC-chemokine binding inhibition at various degrees, suggesting that the profile of HIV-gp120/sCD4 complex binding to CCR5 differs from that of CC-chemokine binding to CCR5.

We finally generated seven clonal populations of $CD4^+$U373-MAGI cells expressing CCR5 with an amino acid substitution which caused significant reduction in the K_D values of either of the three CCR5 inhibitors and examined their susceptibility to $HIV\text{-}1_{BaL}$ infection (Fig. 8*C*). $HIV\text{-}1_{BaL}$ effectively infected $CCR5_{WT}$-expressing cells, however, the susceptibility to $HIV\text{-}1_{BaL}$ infection was greatly reduced in $CCR5_{Y37A}$-, $CCR5_{Y108A}$-, and $CCR5_{I198A}$-expressing cells and that in $CCR5_{G163R}$-, $CCR5_{C178A}$-, $CCR5_{K191A}$-, and $CCR5_{E283A}$-expressing cells was more greatly limited. These data indicate that the mutations examined in this experiment effectively blocked $HIV\text{-}1_{BaL}$ infection, although such mutations, in particular three mutations (G163R, K191A, and I198A), allowed some degrees of sCD4/gp120 binding to $CCR5^+$ cells (Fig. 8*A*).

As noted above, the CC-chemokine binding profile notably differed from the profile of $HIV\text{-}1_{BaL}$ infection susceptibility in $CCR5_{G163R}$- and $CCR5_{I198A}$-expressing cells. Moreover, moderate levels of chemokine binding were seen in $CCR5_{Y108A}$- and $CCR5_{E283A}$-expressing cells, while the least infection occurred in these cells. It should be of note that when we examined what ensued upon the binding of RANTES to $CCR5_{G163R}$-expressing cells, it was found that the level of Ca^{2+} flux that occurred in those cells was comparable to that in $CCR5_{WT}$-expressing cells

following stimulation with RANTES (K Maeda *et al.*, unpublished data).

These data, taken together, suggest that the binding affinity of AVC seen with CCR5 variants generally paralleled the HIV-gp120/sCD4 complex binding affinity to mutant CCR5s, although it is of note that further fine-tuned analysis with greater numbers of CCR5 mutants is required for full understanding of the interactions among HIV-gp120/sCD4 complex, CC-chemokines, and CCR5 inhibitors. The data also suggest that certain conformational changes caused by amino acid substitutions (*e.g.*, at Tyr108, Gly163, or Ile198 residues of CCR5) might substantially reduce HIV-1 infection without significantly affecting physiological CC-chemokine-CCR5 interactions.

DISCUSSION

In the present study, we examined the structural and molecular interactions between CCR5 and three CCR5 inhibitors, aplaviroc (AVC), SCH-C and TAK-779. When we exploited site-directed mutagenesis by generating a panel of mutant CCR5-expressing cells, and determined the K_D values of each CCR5 inhibitor with each mutant CCR5 species, the K_D values compiled corroborated our previous results obtained using the mAb replacement assay (11). We found that the binding affinity of AVC to wild-type CCR5 ($CCR5_{WT}$) was the greatest with a K_D value of 2.9 nM as compared to SCH-C and TAK-779 with K_D values of 16.0 and 30.2, respectively (Table 1). It was also noted that the number of mutations that affected the binding of AVC was greater than in the cases of TAK-779 and SCH-C (Table 1). Moreover, the amino acid substitutions with which AVC turned out to have different K_D values were mostly located in the second extracellular loop (ECL2) and its interface with TM 4 (Gly163), or TM5 (Lys191). By contrast, with regard to SCH-C and TAK-779, no substantially different K_D values were obtained with amino acid substitutions in ECL2 (Table 1). The data suggest that not only the binding interactions but also the molecular size and/or bulkiness of AVC are related to the different numbers of K_D-affecting mutations and different profile of K_D values obtained and that AVC forms substantial hydrophobic contacts with and fits well inside the hydrophobic cavity within CCR5 (Fig. 4*A*). It was also thought that such tight interactions of AVC with residues in ECLs and the interface of extracellular and transmembrane domains of CCR5 are responsible for the greater binding affinity of AVC to CCR5 as compared to other two inhibitors.

It was intriguing that certain amino acids such as Gly163 and Lys191 formed critical hydrogen bond networks in the interaction of AVC and CCR5 (Fig. 3*A-B*). It was thought, therefore, that the amino acid substitutions in such positions dramatically altered the binding affinity of AVC to CCR5. It is also noteworthy that Cys178 of ECL2 is presumed to form a putative disulfide bridge with Cys101 of ECL1 and to be critical for the conformation of CCR5 (34). In the present study, C178A substitution, which should disrupt the putative disulfide bridge and cause significant conformational changes in both ECL1 and ECL2, nullified the CCR5 binding affinity of AVC, but not of SCH-C or TAK-779 (Table 1). In this respect, the lesser interactions of SCH-C and TAK-779 with extracellular domains (Table 1) are likely responsible for the lack of influence of the C178A substitution on the binding affinity of SCH-C and TAK-779, corroborating the notion that mutations in ECL2 did not alter the binding of SCH-C and TAK-779 to CCR5 (Table 1).

Two events are likely involved in the reduced binding of inhibitors to CCR5 with an amino acid substitution(s): i) the alteration of direct interaction, if present, between the amino acid residue and the inhibitor and/or ii) an allosteric effect(s) in which there is a significant conformational change(s) of CCR5 either near or distant from the mutated residue. In this respect, in the present work, we have shown multiple hydrogen bond networks are important for the binding of AVC to CCR5 (Fig. 3*A-B*). Some residues such as K191 directly interact with AVC, and hence mutations that lose this direct interaction are very likely responsible for the loss of binding. The lack of drastic changes in the binding of SCH-C and TAK-779, which are not predicted to directly interact with K191, also supports this inference. G163, however, does not directly bind to AVC but is a critical part of the G163-S180-K191-T195 hydrogen network (Fig. 3*A*). Our molecular modeling, however, indicates that arginine at position 163 does not form

hydrogen bonds with S180 or K191. This alteration in the hydrogen bond network probably changes the shape of the cavity in the ECL2-TM4-TM5 region (an allosteric effect near the mutated residue) and results in reduced binding of AVC to $CCR5_{G163R}$. Mutation at residue 283 might be an example of the one causing an allosteric conformational change(s) distant from the mutated residue. Only AVC is predicted to directly interact with E283, but a E283A mutation results in significant loss of binding for all three inhibitors examined. Thus, it is thought that certain amino acid substitutions reduce the binding of an inhibitor even though they are not directly interacting with the inhibitor. It is also of note that mutations at certain residues directly interacting with an inhibitor do not always cause significant loss of binding if CCR5 does not undergo a conformational change(s) or takes an alternate conformation that is not unfavorable for inhibitor binding.

Since a crystal structure of CCR5 is not available, unlike other targets for intervention of HIV infection including HIV reverse transcriptase (36), in the present study, in an attempt to conduct structural analyses of the interactions of CCR5 inhibitors with various mutant CCR5 species, an initial structural model of CCR5 was generated using homology modeling based on the crystal structure of bovine rhodopsin (23). The present approach of combining the site-directed mutagenesis-based data (Table 1) and molecular modeling should be a valuable strategy for gaining structural insights for membrane-bound proteins for which X-ray crystal structures are not as yet available. The CCR5-inhibitor complex structures were defined by iterative optimization of CCR5 and inhibitor structures. Mutated CCR5 structures were also defined and optimized based on the wild type CCR5 structure, and minimized structures of various CCR5 mutants were used as starting structures for obtaining docked complexes of mutated CCR5 with inhibitors. It is of note that in the present study, our modeling study was combined and fine-tuned with the results of the saturation binding assay using a panel of mutant CCR5-expressing cells and tritiated CCR5 inhibitors and the resultant configuration and orientation of inhibitors docked within the hydrophobic cavity of CCR5 yielded a consistent analysis of the structure-activity data. The conformations of CCR5 without an inhibitor and CCR5 bound to an inhibitor are likely to be substantially different from each other since conformational changes are expected to occur upon inhibitor binding to CCR5. Thus, the conformational flexibility of both inhibitors and CCR species were taken into account in our analysis. In this regard, our ongoing analyses of binding affinity profiles using different ^{3}H-labeled CCR5 inhibitors and an expanded panel of mutant CCR5-expressing cell lines should further illuminate the intramolecular and intermolecular interactions of CCR5 and CCR5 inhibitors.

We also examined the binding profile of CCR5 inhibitors when one inhibitor was added to CCR5-overexpressing cells, followed by the addition of the second inhibitor (Fig. 7). Interestingly, when AVC first bound to CCR5 and SCH-C or TAK-779 was subsequently added, both SCH-C and TAK-779 only partially displaced AVC (Fig. 7*A-B*). However, when SCH-C or TAK-779 first bound to CCR5 and AVC was subsequently added, SCH-C and TAK-779 were substantially displaced by AVC (Fig. 7*C-D*). This ineffective displacement of AVC once bound to $CCR5_{WT}$ by SCH-C and TAK-779 could be explained by the difference of their K_D values (2.9 nM for AVC, 16 nM for SCH-C, and 30.2 nM for TAK-779 as illustrated in Table 1). However, it is of note that both SCH-C and TAK-779 failed to displace AVC even with very high concentrations: 3,333-fold (10 μM; Fig. 7*A*) and 20,833-fold (62.5 μM; Fig. 7*B*), respectively, greater than the ^{3}H-AVC concentration (3 nM). Thus, only the difference in K_D values among the three inhibitors unlikely fully explains the failure of AVC replacement by SCH-C and TAK-779. In this regard, a possible explanation is that AVC induces a series of significant conformational changes in CCR5 and, upon the completion of its stable lodging within the hydrophobic cavity within $CCR5_{WT}$, the binding and/or entry into CCR5 of the second inhibitor is hindered and the interaction between AVC and the second inhibitor added is no longer merely competitive. Although the data of displacement experiments using two CCR5 inhibitors discussed above may not offer clear mechanistic explanation at present due to the limitation of the currently available methodologies, the data may have a clinical relevance in the future since more than one

CCR5 inhibitors may be simultaneously administered when multiple CCR5 inhibitors are introduced in the therapy of AIDS. It is also noteworthy that the tight CCR5 binding profile of AVC is presumably related to the extensive and prolonged CCR5 occupancy observed in phytohemagglutinin-activated peripheral blood mononuclear cells ($T_{1/2}$ ~9 hr) (12) and in circulating lymphocytes in HIV-1-negative and HIV-1-positive individuals ($T_{1/2}$ of 69-152 hr depending on different AVC doses), a potentially favorable feature which could enable once daily (*QD*) or twice daily (*BID*) administration of AVC.

In the present study, we observed that amino acid mutations within the transmembrane domains such as Y108A, G163R, and I198A exerted only minimal or moderate effects on the binding of CC-chemokines to CCR5 (Fig. 8*B*), while they caused a substantial reduction in HIV-1 gp120/CD4 complex binding to CCR5 (Fig. 8*A*) and a more drastic reduction in the susceptibility to HIV-1 infection (Fig. 8*C*). It is possible that the molecular size of gp120/sCD4 complex is far greater and its interactions with CCR5 are more extensive compared to the case of CC-chemokines, and therefore, the process for establishing HIV-1 infection is more extensively affected by such amino acid substitutions in comparison to CCR5 binding of CC-chemokines and the ensuing signal transduction. In this regard, a large body of literature has shown that CCR5 regions to which HIV-1's envelope glycoproteins bind are functionally and structurally quite different from those to which CC-chemokines bind (19-21,32,33). Wu *et al.* and Lee *et al.* demonstrated that a group of CCR5's NH_2-terminus-specific monoclonal antibodies did not block the binding of or Ca^{2+} flux induction by CC-chemokines, although ECL2-specific monoclonal antibodies effectively block the binding of CC-chemokines and their Ca^{2+} flux induction (20,21). Navenot *et al.* subsequently confirmed these notions and further demonstrated that a CCR5 chimera with the NH_2-terminus of CXCR2 bound MIP-1α with an affinity similar to that of $CCR5_{WT}$ (33). In contrast, both NH_2-terminus- and ECL2-specific mAbs reportedly blocked efficiently the binding of gp120 to CCR5 although the latter mAbs caused superior inhibition (20,21). These previously published data strongly suggest that the interactions of CCR5 with HIV-1-glycoproteins involve multiple CCR5 domains and consist of more complex processes while those with CC-chemokines involve fewer CCR5 domains and potentially fewer processes. Thus, this implies that the intervention of HIV-1 infection without interrupting physiological CC-chemokine/CCR5 interactions should be feasible. Indeed, AVC does not potently block the physiologic CC-chemokine/CCR5 interactions, although it highly efficiently suppresses the infection of HIV-1 with IC_{50} values of subnanomolar concentrations (11).

Taken together, mutations associated with AVC binding to CCR5 decreased gp120 binding to CCR5 and the susceptibility to HIV-1 infection, while mutations in TM4 and TM5 that also decreased gp120 binding and HIV-1 infectivity had less effects on the binding of CC-chemokines, suggesting that CCR5 inhibition targeting appropriate regions might render the inhibition highly HIV-1-specific, preserving the CC chemokine-CCR5 interactions. The present data should not only help design more potent and HIV-1-specific CCR5 inhibitors, but also should give new insights into the dynamics of CC-chemokine-CCR5 interactions and the mechanisms of CCR5 involvement in the process of cellular entry of HIV-1.

REFERENCES

1. Fauci, A. S. (2003) *Nat Med* **9**(7), 839-843
2. Mitsuya, H., and Erickson, J. (1999) Discovery and development of antiretroviral therapeutics for HIV infection. In: Merigan, T. C., Bartlet, J. G., and Bolognesi, D. (eds). *Textbook of AIDS Medicine*, Williams & Wilkins, Baltimore
3. Siliciano, J. D., Kajdas, J., Finzi, D., Quinn, T. C., Chadwick, K., Margolick, J. B., Kovacs, C., Gange, S. J., and Siliciano, R. F. (2003) *Nat Med* **9**(6), 727-728

4. Richman, D. D. (2001) *Nature* **410**(6831), 995-1001
5. Department of Health and Human Services (DHHS). (2005) Guidelines for the Use of Antiretroviral Agents in HIV-1-Infected Adults and Adolescents.
6. Raport, C. J., Gosling, J., Schweickart, V. L., Gray, P. W., and Charo, I. F. (1996) *J Biol Chem* **271**(29), 17161-17166
7. Alkhatib, G., Combadiere, C., Broder, C. C., Feng, Y., Kennedy, P. E., Murphy, P. M., and Berger, E. A. (1996) *Science* **272**(5270), 1955-1958
8. Deng, H., Liu, R., Ellmeier, W., Choe, S., Unutmaz, D., Burkhart, M., Di Marzio, P., Marmon, S., Sutton, R. E., Hill, C. M., Davis, C. B., Peiper, S. C., Schall, T. J., Littman, D. R., and Landau, N. R. (1996) *Nature* **381**(6584), 661-666
9. Trkola, A., Dragic, T., Arthos, J., Binley, J. M., Olson, W. C., Allaway, G. P., Cheng-Mayer, C., Robinson, J., Maddon, P. J., and Moore, J. P. (1996) *Nature* **384**(6605), 184-187.
10. Wu, L., Gerard, N. P., Wyatt, R., Choe, H., Parolin, C., Ruffing, N., Borsetti, A., Cardoso, A. A., Desjardin, E., Newman, W., Gerard, C., and Sodroski, J. (1996) *Nature* **384**(6605), 179-183.
11. Maeda, K., Nakata, H., Koh, Y., Miyakawa, T., Ogata, H., Takaoka, Y., Shibayama, S., Sagawa, K., Fukushima, D., Moravek, J., Koyanagi, Y., and Mitsuya, H. (2004) *J Virol* **78**(16), 8654-8662
12. Nakata, H., Maeda, K., Miyakawa, T., Shibayama, S., Matsuo, M., Takaoka, Y., Ito, M., Koyanagi, Y., and Mitsuya, H. (2005) *J Virol* **79**(4), 2087-2096
13. Baba, M., Nishimura, O., Kanzaki, N., Okamoto, M., Sawada, H., Iizawa, Y., Shiraishi, M., Aramaki, Y., Okonogi, K., Ogawa, Y., Meguro, K., and Fujino, M. (1999) *Proc Natl Acad Sci U S A* **96**(10), 5698-5703
14. Strizki, J. M., Xu, S., Wagner, N. E., Wojcik, L., Liu, J., Hou, Y., Endres, M., Palani, A., Shapiro, S., Clader, J. W., Greenlee, W. J., Tagat, J. R., McCombie, S., Cox, K., Fawzi, A. B., Chou, C. C., Pugliese-Sivo, C., Davies, L., Moreno, M. E., Ho, D. D., Trkola, A., Stoddart, C. A., Moore, J. P., Reyes, G. R., and Baroudy, B. M. (2001) *Proc Natl Acad Sci U S A* **98**(22), 12718-12723.
15. Gribble, G. W. (1975) *JCS Chem. Comm.*, 535-541
16. Evans, E. A. (1974) Tritium and its compounds. In., J. Willey and Sons, New York
17. Maeda, K., Yoshimura, K., Shibayama, S., Habashita, H., Tada, H., Sagawa, K., Miyakawa, T., Aoki, M., Fukushima, D., and Mitsuya, H. (2001) *J Biol Chem* **276**(37), 35194-35200.
18. Maeda, Y., Foda, M., Matsushita, S., and Harada, S. (2000) *J Virol* **74**(4), 1787-1793
19. Siciliano, S. J., Kuhmann, S. E., Weng, Y., Madani, N., Springer, M. S., Lineberger, J. E., Danzeisen, R., Miller, M. D., Kavanaugh, M. P., DeMartino, J. A., and Kabat, D. (1999) *J Biol Chem* **274**(4), 1905-1913.
20. Wu, L., LaRosa, G., Kassam, N., Gordon, C. J., Heath, H., Ruffing, N., Chen, H., Humblias, J., Samson, M., Parmentier, M., Moore, J. P., and Mackay, C. R. (1997) *J Exp Med* **186**(8), 1373-1381
21. Lee, B., Sharron, M., Blanpain, C., Doranz, B. J., Vakili, J., Setoh, P., Berg, E., Liu, G., Guy, H. R., Durell, S. R., Parmentier, M., Chang, C. N., Price, K., Tsang, M., and Doms, R. W. (1999) *J Biol Chem* **274**(14), 9617-9626
22. Maeda, Y., Venzon, D. J., and Mitsuya, H. (1998) *J Infect Dis* **177**(5), 1207-1213.
23. Palczewski, K., Kumasaka, T., Hori, T., Behnke, C. A., Motoshima, H., Fox, B. A., Le Trong, I., Teller, D. C., Okada, T., Stenkamp, R. E., Yamamoto, M., and Miyano, M. (2000) *Science* **289**(5480), 739-745.
24. Halgren, T. A., Murphy, R. B., Friesner, R. A., Beard, H. S., Frye, L. L., Pollard, W. T., and Banks, J. L. (2004) *J Med Chem* **47**(7), 1750-1759
25. Xiang, Z., and Honig, B. (2001) *J Mol Biol* **311**(2), 421-430
26. Kaminski, G. A., Friesner, R. A., Tirado-Rives, J., and Jorgensen, W. J. (2001) *J. Phys. Chem. B* **105**, 6474-6487
27. Friesner, R. A., Banks, J. L., Murphy, R. B., Halgren, T. A., Klicic, J. J., Mainz, D. T., Repasky, M. P., Knoll, E. H., Shelley, M., Perry, J. K., Shaw, D. E., Francis, P., and Shenkin, P. S. (2004) *J Med Chem* **47**(7), 1739-1749
28. Exner, T. E., Keil, M., Moeckel, G., and Brickmann, J. (1998) *J. Mol. Model.* **4**, 340-343

29. Viswanadhan, V. N., Ghose, A. K., Revankar, G. R., and Robins, R. K. (1989) *J. Chem. Inf. Comput. Sci.* **29**, 163-172
30. Dragic, T., Trkola, A., Thompson, D. A., Cormier, E. G., Kajumo, F. A., Maxwell, E., Lin, S. W., Ying, W., Smith, S. O., Sakmar, T. P., and Moore, J. P. (2000) *Proc Natl Acad Sci U S A* **97**(10), 5639-5644
31. Tsamis, F., Gavrilov, S., Kajumo, F., Seibert, C., Kuhmann, S., Ketas, T., Trkola, A., Palani, A., Clader, J. W., Tagat, J. R., McCombie, S., Baroudy, B., Moore, J. P., Sakmar, T. P., and Dragic, T. (2003) *J Virol* **77**(9), 5201-5208
32. Dragic, T., Trkola, A., Lin, S. W., Nagashima, K. A., Kajumo, F., Zhao, L., Olson, W. C., Wu, L., Mackay, C. R., Allaway, G. P., Sakmar, T. P., Moore, J. P., and Maddon, P. J. (1998) *J Virol* **72**(1), 279-285.
33. Navenot, J. M., Wang, Z. X., Trent, J. O., Murray, J. L., Hu, Q. X., DeLeeuw, L., Moore, P. S., Chang, Y., and Peiper, S. C. (2001) *J Mol Biol* **313**(5), 1181-1193.
34. Blanpain, C., Lee, B., Vakili, J., Doranz, B. J., Govaerts, C., Migeotte, I., Sharron, M., Dupriez, V., Vassart, G., Doms, R. W., and Parmentier, M. (1999) *J Biol Chem* **274**(27), 18902-18908
35. Govaerts, C., Bondue, A., Springael, J. Y., Olivella, M., Deupi, X., Le Poul, E., Wodak, S. J., Parmentier, M., Pardo, L., and Blanpain, C. (2003) *J Biol Chem* **278**(3), 1892-1903
36. Sarafianos, S. G., Das, K., Hughes, S. H., and Arnold, E. (2004) *Curr Opin Struct Biol* **14**(6), 716-730

ACKNOWLEDGEMENTS

The authors thank Steve LaFon, James Demarest, Alphonso Nillas, Larry Boone, Yashuhiro Koh, Yosuke Maeda, and Philip Yin for helpful discussion and/or critical reading of the manuscript. The authors also thank the Center for Information Technology, National Institutes of Health, for providing computational resources. This work was supported in part by the Intramural Research Program of Center for Cancer Research, National Cancer Institute, National Institutes of Health and in part by a Grant-in-aid for Scientific Research (Priority Areas) from the Ministry of Education, Culture, Sports, Science, and Technology of Japan (Monbu-Kagakusho), a Grant for Promotion of AIDS Research from the Ministry of Health, Welfare, and Labor of Japan (Kosei Rohdosho: H15-AIDS-001), and the Grant to the Cooperative Research Project on Clinical and Epidemiological Studies of Emerging and Re-emerging Infectious Diseases (Renkei Jigyo: No. 78, Kumamoto University) of Monbu-Kagakusho.

FIGURE LEGENDS

Fig. 1. Structures of aplaviroc (AVC), TAK-779, and SCH-C.

Fig. 2. Hydrophobic cavities identified within CCR5. Six hydrophobic cavities are identified within human CCR5, defined using MOLCAD (Sybyl 7.0). Note the largest hydrophobic cavity (red arrow head) that is likely to accommodate a molecule of the size of AVC and other CCR5 inhibitors and is in the region implicated to have greatest effects on K_D values (see mutagenesis-based results in Table 1).

Fig. 3. Hydrogen bond networks within CCR5 critical for AVC binding to CCR5. The structure of CCR5-AVC complex was defined with iterative structural refinement using docking and homology modeling. Only polar hydrogen atoms are shown. Panel *A*, An intramolecular hydrogen bond network comprised of Gly163, Ser180, Lys191, and Thr195 is seen. Gly163 is located in TM4, Ser180 in ECL2, and Lys191 and Thr195 in TM5. The structural analyses illustrate the presence of intermolecular hydrogen bonds of AVC with residues Cys178, Ser180, Lys191, and Thr195 of CCR5. Panel *B*, An intramolecular hydrogen bond network is seen involving Tyr37, Glu283, Met287, and Tyr108. Tyr37 is located in TM1, Tyr108 in TM3, and Glu283 and Met287 in TM7. Glu283 forms hydrogen bond interactions with the hydroxymethyl of AVC. Intramolecular hydrogen bonds are shown in pink, and the intermolecular hydrogen bonds in green. Note that the hydrogen bond networks spanning multiple domains should maintain the optimal shape of the cavity for the binding of AVC (Fig. 4*A-B*). Panel *C*, The predicted van der Waals contact between AVC and CCR5 residues Lys191 and Ile198. AVC is shown in green spheres, whereas Lys191 and Ile198 in magenta.

Fig. 4. The configuration of aplaviroc within CCR5. Panel *A*, AVC lodged within the binding cavity of CCR5. The CCR5 cavity was defined with its lipophilic potential using MOLCAD. The region near the extracellular domain has some hydrophilic character (red arrow head), whereas the rest of the cavity is mostly lipophilic. The carboxyl and hydroxymethyl of AVC interact with the hydrophilic regions of CCR5, whereas the rest of AVC interacts with the lipophilic regions of CCR5. Panel *B*, A docked structure of AVC (tube representation) bound to CCR5, illustrating the relative location of AVC within CCR5. Important binding site residues of CCR5 are shown in wires. Polar hydrogens are only shown. Note that TM 1, 2, and 3 are towards the viewer from the plane and TM 6 and 7 are away from the viewer behind the plane.

Fig. 5. Interactions of SCH-C with CCR5 residues. Panel *A*, The configuration of SCH-C (shown in CPK) obtained with mutagenesis-based data (Table 1) combined with structural analyses. CCR5 residue orientations (shown in tubes) vary from that in Fig. 4 since conformational flexibility of receptors during docking of each inhibitor was taken into account. Panel *B*, Tyr37 forms hydrogen bonding interactions with SCH-C, and hence Y37A mutation reduces the binding affinity of SCH-C with CCR5. Note the location of Tyr108 and compare its corresponding location for the complex with TAK-779. SCH-C is shown in tubes and CCR5 residues in wires. Only polar hydrogens are shown in panel *A* and *B*. The molecules are colored by atom types (carbon, grey; oxygen, red; nitrogen, blue; hydrogen, cyan; sulfur, yellow; bromine, green). Panel *C*, van der Waals interactions of SCH-C (green) with Lys191 and Ile198 (magenta). There is tight hydrophobic binding of SCH-C with Ile198. Unlike AVC, Lys191 does not form significant interactions with SCH-C.

Fig. 6. Interactions of TAK-779 with CCR5 residues. Panel *A*, The configuration of TAK-779 within the CCR5 binding pocket. Panel *B*, Tyr37 forms a hydrogen bonding interaction with TAK-779. Note the orientation of Tyr108 in comparison to CCR5's complex with SCH-C. Tyr108 forms π-π and hydrogen bond interactions with TAK-779 and represents a critical residue in agreement with the mutagenesis-based results (Table 1). Only polar hydrogens are shown. The molecules are colored by atom types (carbon, grey; oxygen, red; nitrogen, blue; hydrogen, cyan; sulfur, yellow).

Fig. 7. Interactions between CCR5 inhibitors in relation to CCR5. $CCR5_{WT}$-CHO cells were exposed to ^{3}H-AVC (3 nM; panel *A* and *B*), ^{3}H-SCH-C (3 nM; panel *C*), or ^{3}H-TAK-779 (10 nM; panel *D*), for 15 min, followed by the exposure to various concentrations (from 1 nM to 62.5 μM) of unlabelled SCH-C (panel *A*), TAK-779 (panel *B*), or AVC (panel *C* and *D*) for 30 min. The cells were then thoroughly washed, lysed, and the radioactivity of the lysates was counted. All experiments were performed in duplicate and the data shown are mean values ± SD. The amounts of ^{3}H-CCR5 inhibitor bound to the cells are shown as mean % control values (each control value was obtained without an indicated unlabelled CCR5 inhibitor).

Fig. 8. Effects of amino acid substitutions in CCR5 on sCD4/gp120 binding, HIV infection, and CC-chemokine binding. Panel *A*, Profiles of the binding of $sCD4/gp120_{YU2}$ complex to various $CCR5_{MT}$ species overexpressing CHO cells. All values were normalized with the CCR5 expression level of each $CCR5_{MT}$ compared to that of $CCR5_{WT}$ (See Experimental Procedures). Panel *B*, Profiles of the binding of ^{125}I-RANTES, ^{125}I-MIP-1α, and ^{125}I-MIP-1β to various $CCR5_{MT}$-expressing CHO cell preparations. All values were normalized with the CCR5 expression level of each $CCR5_{MT}$ compared to that of $CCR5_{WT}$. All assays were performed in duplicate or triplicate. Panel *C*, The susceptibility of various $CCR5_{MT}$-overexpressing U373-MAGI cells. For testing each of $CCR5_{MT}$-overexpressing cell preparations, multiple clones were examined. In each set of experiments, $CCR5_{WT}$-clone #1 (solid column) served as a standard (100%).

Table 1. Binding affinity of CCR5 inhibitors to mutant CCR5s

Mutant CCR5 overexpressed on CHO cells		K_D value[a] (nM) Aplaviroc	SCH-C	TAK-779	gp120/sCD4 binding[b] (%control)
wild type		2.9 ± 1.0	16.0 ± 1.5	30.2 ± 7.6	100 ± 13.3
D11A	*NH_2- terminus*	3.0 ± 0.6	12.4 ± 2.0	24.5 ± 3.7	35.4 ± 4.7
Y37A	*TM1*	7.9 ± 0.9	**>200**	**98.9 ± 11.5**	35.4 ± 3.7
Y108A		**19.8 ± 4.4**[c]	11.8 ± 1.1	**>200**	13.2 ± 1.0
F112L		4.0 ± 2.6	30.0 ± 6.4	33.0 ± 7.2	
F112Y	*TM3*	6.8 ± 1.1	35.8 ± 7.6	28.5 ± 3.1	111 ± 6.9
F113A		**13.3 ± 2.3**	43.8 ± 6.3	32.7 ± 3.3	
F113Y		8.6 ± 3.4	45.3 ± 12.1	32.4 ± 3.0	
G163A	*TM4-ECL2*	8.0 ± 4.2	25.0 ± 8.2	24.0 ± 5.9	
G163R		**>200**	46.3 ± 16.5	88.3 ± 22.9	34.1 ± 5.4
R168A		**13.2 ± 3.3**	21.0 ± 8.1	43.0 ± 4.7	
KE171AA		2.8 ± 0.1	34.8 ± 6.8	30.5 ± 0.7	29.6 ± 2.2
C178A		**>200**	27.1 ± 4.4	34.5 ± 3.5	20.9 ± 1.0
S180A		5.7 ± 1.2	31.8 ± 14.4	18.2 ± 3.2	
S180T	*ECL2*	1.5 ± 0.6	25.4 ± 6.8	41.0 ± 3.8	101 ± 15.0
S180E		**13.9 ± 1.7**	16.5 ± 2.2	25.0 ± 3.5	51.6 ± 1.1
YS184AA		2.0 ± 0.8	21.3 ± 5.0	28.0 ± 2.5	
YSQY184AAA		2.0 ± 0.6	14.9 ± 0.6	32.3 ± 5.8	
QY186AA		2.8 ± 0.5	14.7 ± 8.8	35.2 ± 5.8	
Q188A		6.6 ± 1.4	23.8 ± 1.5	37.9 ± 2.5	
WKNF190del		**>200**	**49.2 ± 1.7**	80.1 ± 16.7	
K191A		**>200**	26.5 ± 7.1	35.0 ± 3.8	45.7 ± 0.6
K191R	*ECL2-TM5*	**9.0 ± 5.6**	34.1 ± 19.1	47.1 ± 8.8	
K191N		**14.2 ± 1.1**	35.8 ± 9.2	35.1 ±9.3	
K197A	*TM5*	**9.2 ± 4.3**	16.8 ± 2.9	14.7 ± 1.1	
I198A		**24.6 ± 4.8**	**52.4 ± 3.0**	54.9 ± 6.9	51.7 ± 3.0
Y251A	*TM6*	**36.5 ± 9.5**	21.5 ± 8.6	43.0 ± 4.5	14.5 ± 0.7
E283A		**>200**	**>200**	**>200**	4.3 ± 0.6
M287A	*TM7*	6.8 ± 2.3	28.0 ± 9.1	39.8 ± 7.5	104 ± 3.9
M287E		**14.8 ± 1.7**	32.2 ± 4.2	53.1 ± 3.7	22.0 ± 0.8

[a] K_D values were determined using saturation binding assays (Experimental Procedures).

[b] gp120/sCD4 binding affinity to $CCR5_{MT}$ is shown by % control (see Experimental Procedures for reference), the data is also shown in Figure 8*A*

[c] K_D values more than 3-fold compared to that with $CCR5_{WT}$ are shown in bold. All K_D values were determined on multiple occasions (twice to 6 times). Considering the standard deviation for the wild-type, and other mutations, a 3-fold difference was seen to be statistically significant.

Figure 1

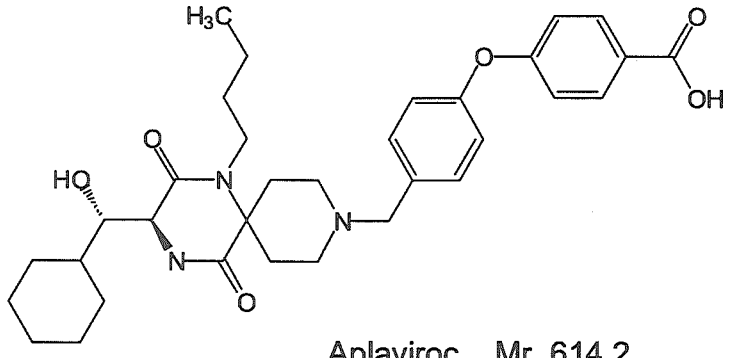

Aplaviroc Mr. 614.2

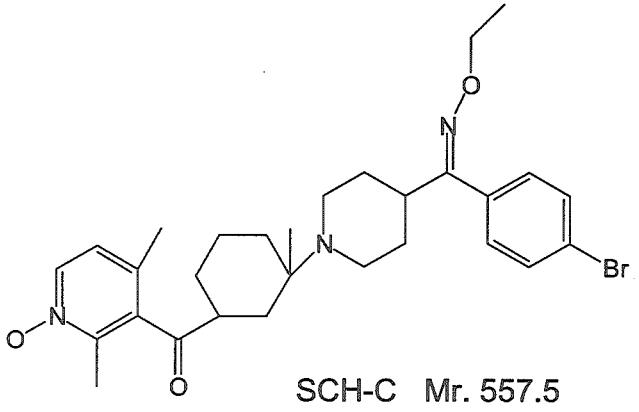

SCH-C Mr. 557.5

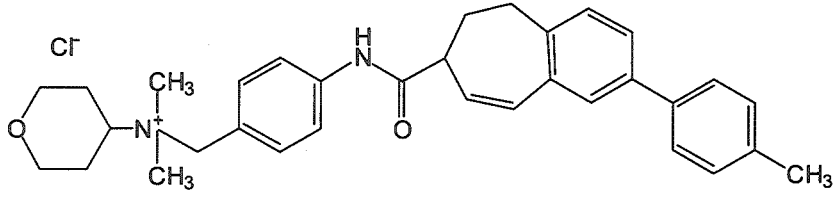

TAK-779 Mr. 531.1

Figure 2

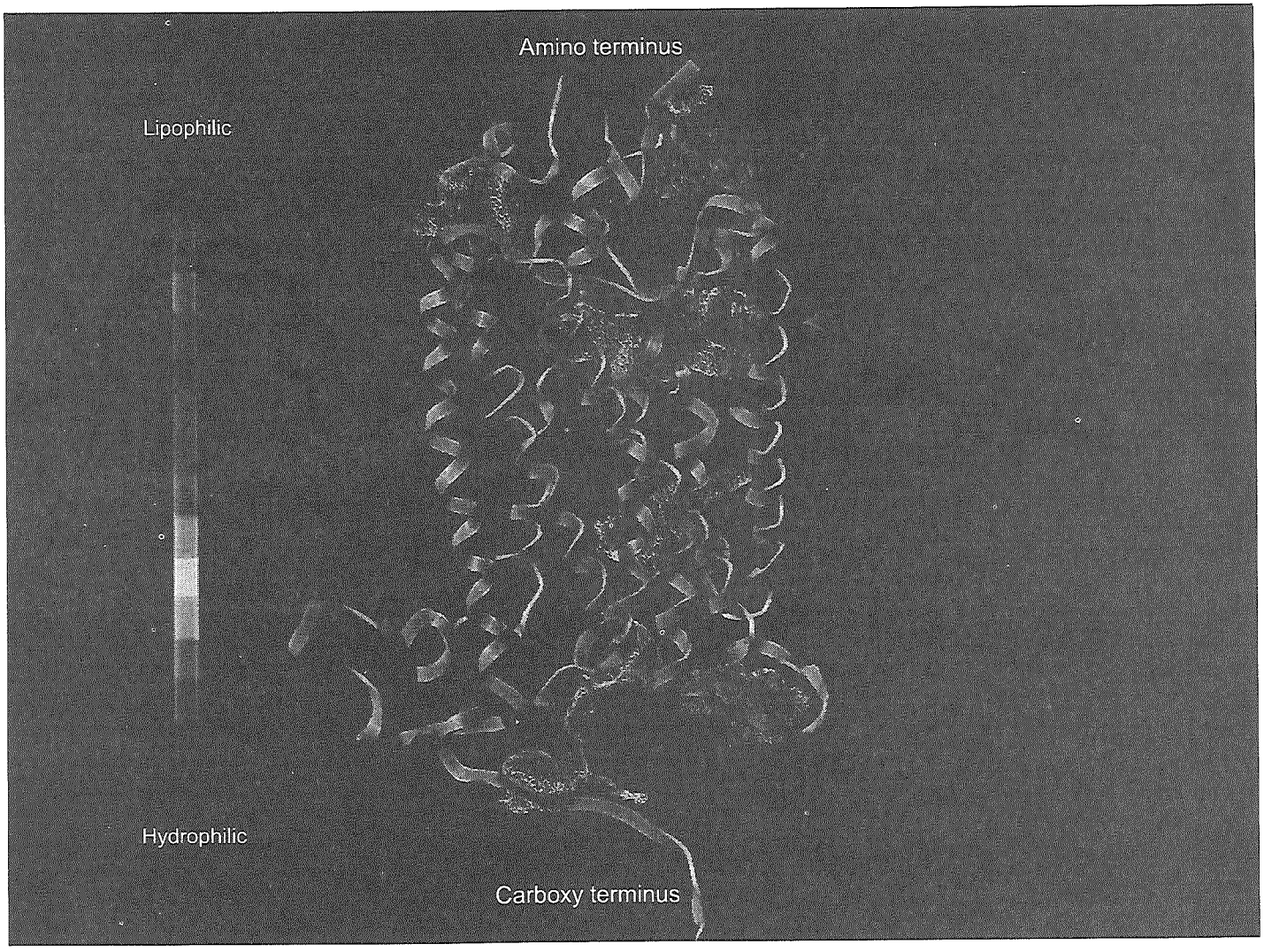

Figure 3

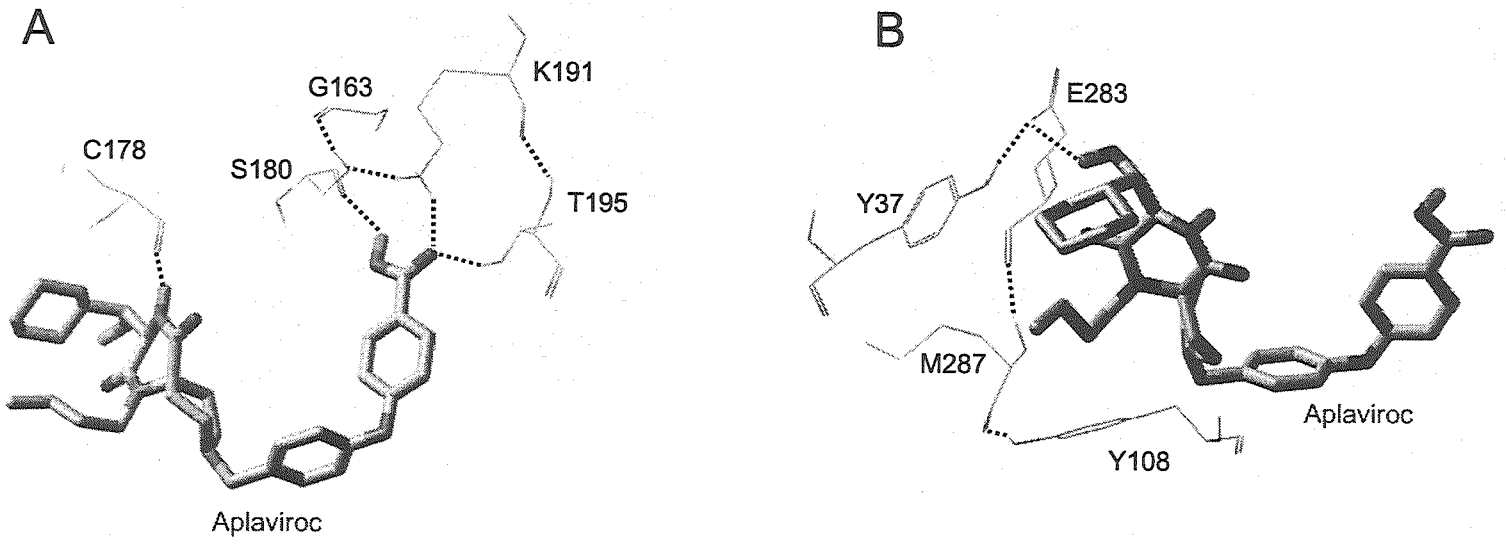
A
K191
G163
C178
S180
T195
Aplaviroc
B
E283
Y37
M287
Aplaviroc
Y108

Figure 3

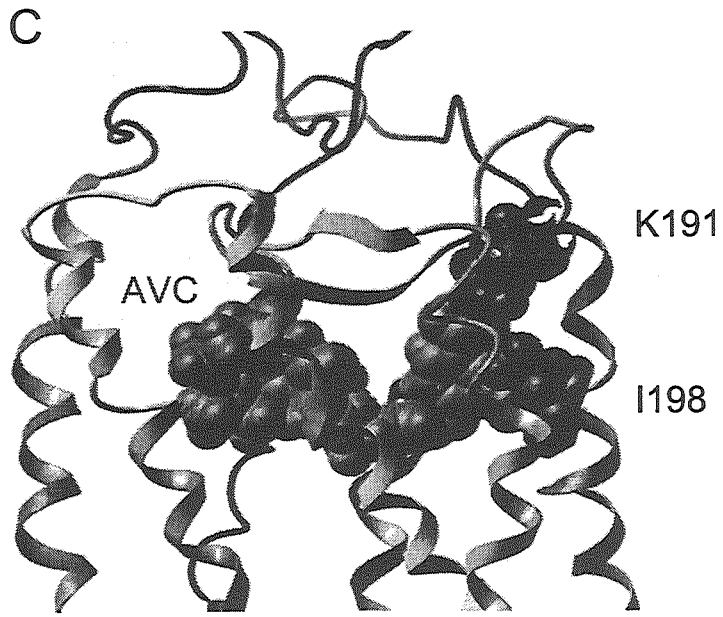

Figure 4

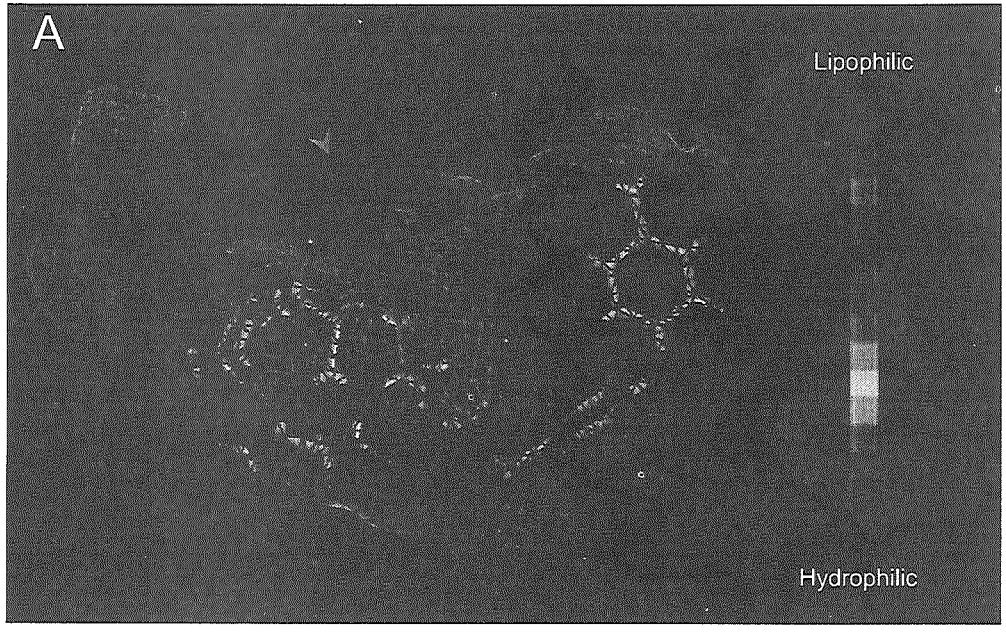
A
Lipophilic
Hydrophilic

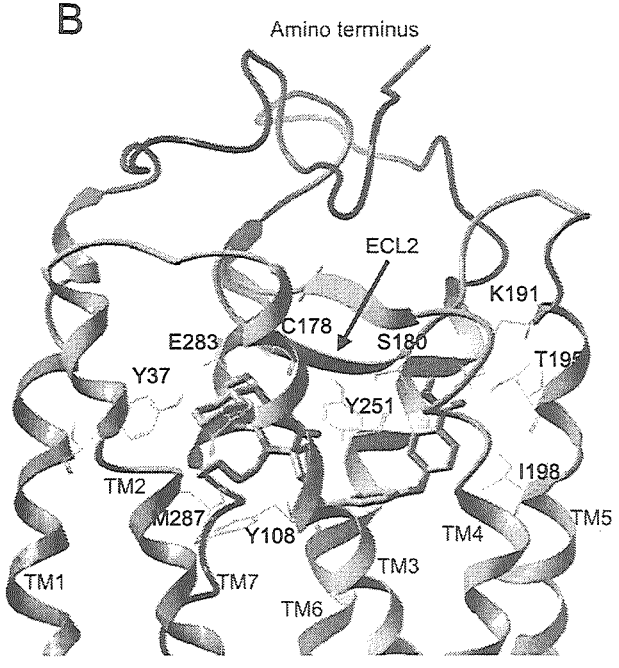
B
Amino terminus
ECL2
K191
C178
S180
E283
T195
Y37
Y251
I198
TM2
M287
Y108
TM4
TM5
TM3
TM1
TM7
TM6

Figure 5

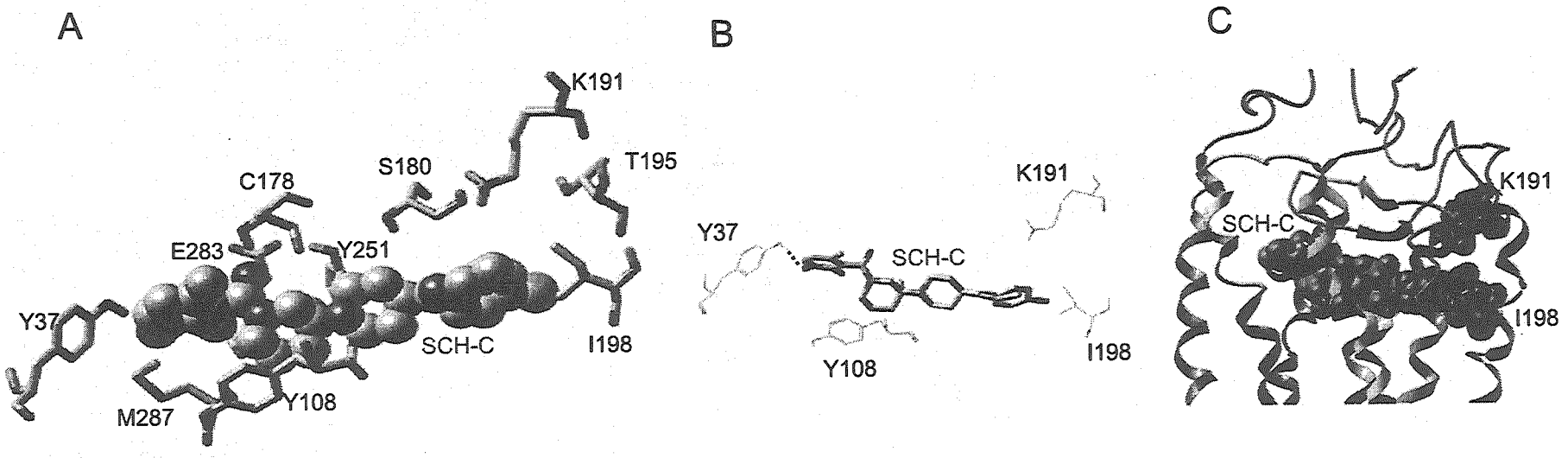
A
K191
S180
T195
C178
E283
Y251
Y37
SCH-C
I198
M287
Y108
B
K191
Y37
SCH-C
Y108
I198
C
K191
SCH-C
I198

Figure 6

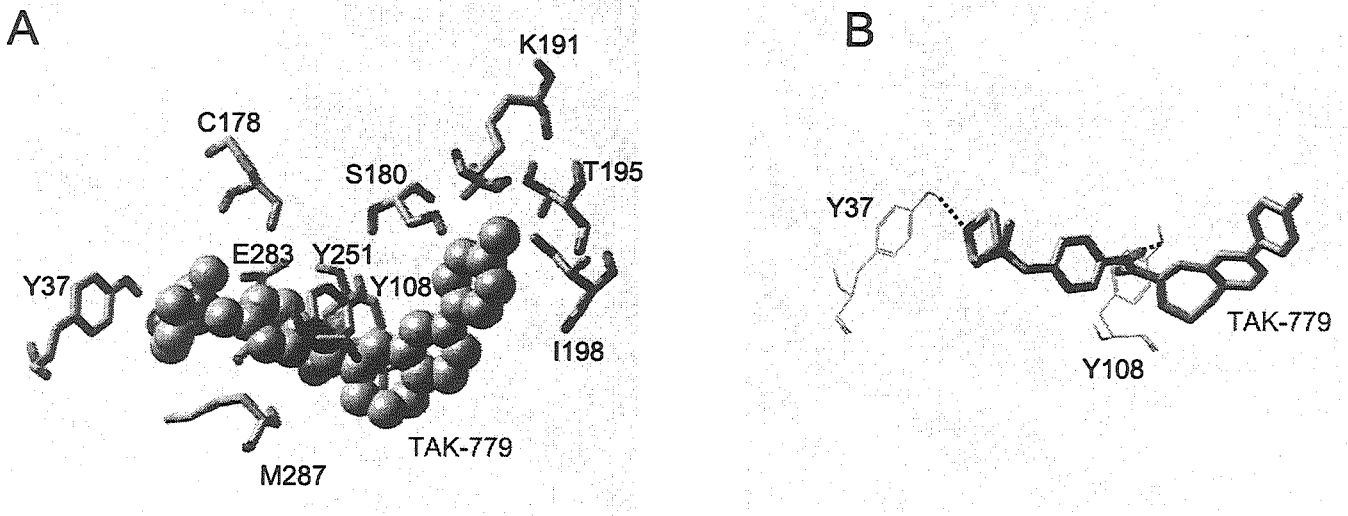
A
K191
C178
S180
T195
E283
Y251
Y37
Y108
I198
TAK-779
M287
B
Y37
TAK-779
Y108

Figure 7

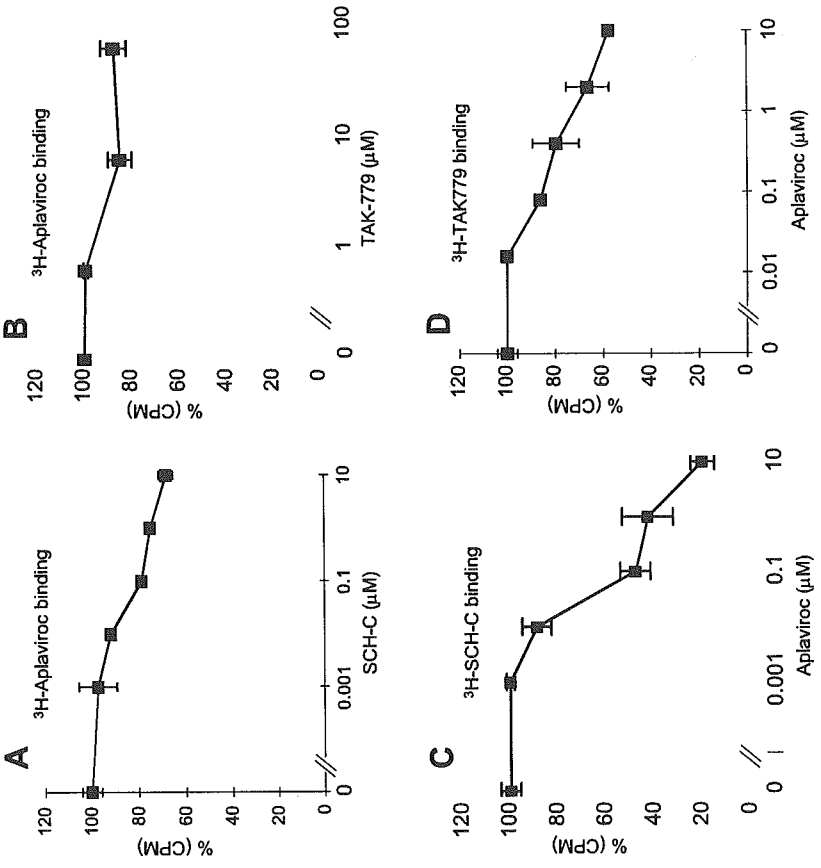
A
3H-Aplaviroc binding
% (CPM)
SCH-C (μM)
B
3H-Aplaviroc binding
% (CPM)
TAK-779 (μM)
C
3H-SCH-C binding
% (CPM)
Aplaviroc (μM)
D
3H-TAK779 binding
% (CPM)
Aplaviroc (μM)

Figure 8

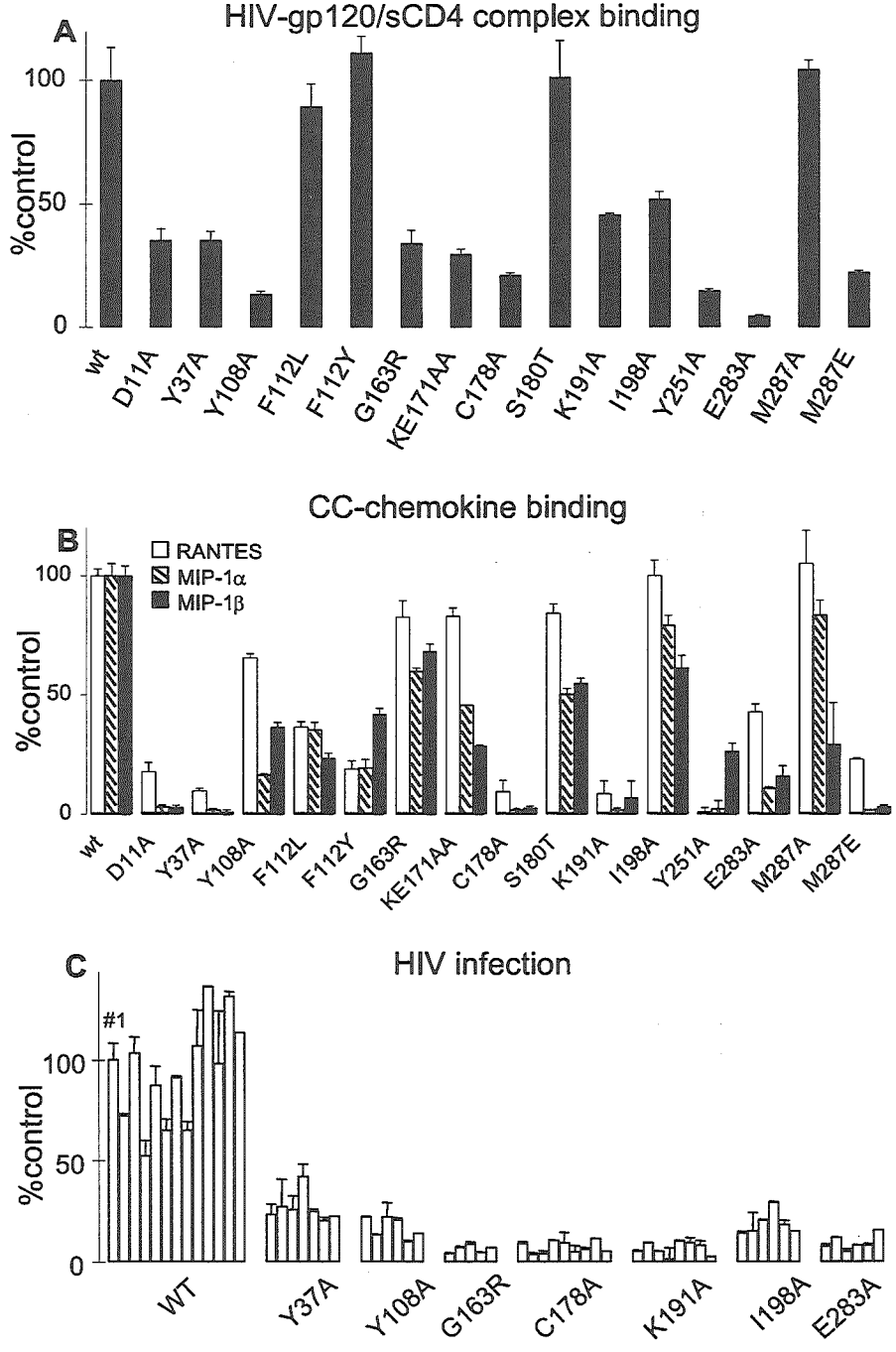
A
HIV-gp120/sCD4 complex binding
%control
100
50
0
wt
D11A
Y37A
Y108A
F112L
F112Y
G163R
KE171AA
C178A
S180T
K191A
I198A
Y251A
E283A
M287A
M287E
B
CC-chemokine binding
RANTES
MIP-1α
MIP-1β
%control
100
50
0
wt
D11A
Y37A
Y108A
F112L
F112Y
G163R
KE171AA
C178A
S180T
K191A
I198A
Y251A
E283A
M287A
M287E
C
HIV infection
#1
%control
100
50
0
WT
Y37A
Y108A
G163R
C178A
K191A
I198A
E283A

平成15－17年度　厚生労働科学研究費補助金エイズ対策研究事業
「免疫賦活を応用したHIV感染症の治療開発に関する研究」班
総合研究報告書

発行日　2006年3月31日

発行者　主任研究者　岡　慎一

発行所　研究班事務局
国立国際医療センター病院
エイズ治療・研究開発センター
〒162-8655　東京都新宿区戸山1-21-1